

Strategies for employing surface plasmons in a near field transmission optical readout system

Choon How Gan^{a)} and Greg Gbur

Department of Physics and Optical Science, University of North Carolina at Charlotte, Charlotte, North Carolina 28223, USA

(Received 5 July 2007; accepted 2 September 2007; published online 26 September 2007)

Strategies to manipulate the surface plasmon-enhanced transmission in a near field optical readout system to achieve super-resolution are investigated. Our numerical simulations demonstrate that modulation and confinement of the plasmon-assisted effects in the readout system can be accomplished through appropriately placed “plasmon pits.” It is found from the simulation results that using short metallic strips embedded in a thin dielectric film instead of a thin metal film for the data structure can aid in localizing the plasmonic effects, thereby improving the resolution of the readout system. In the simulated geometries considered, resolution up to $\sim\lambda/5$ is achievable.

© 2007 American Institute of Physics. [DOI: 10.1063/1.2789388]

The drive for increased optical data storage capacity has stimulated much interest in the area of near field optical readout, an approach that offers the capability for operation beyond the diffraction limit. Several techniques have been proposed, examples of which include achieving super-resolution with a super-resolution near field structure,^{1,2} with thermoreversible organic materials³ and with thermoelectric materials.⁴ Since the observation of surface plasmon-enhanced transmission through subwavelength apertures in metal plates,^{5,6} there have been increased interests to apply plasmonic effects to various optical nanotechnologies.⁷ Recently, a near field optical readout system that manipulates surface plasmons by means of “plasmon pits” was investigated.⁸ The role of these plasmon pits was to facilitate the light-plasmon coupling and to confine the fields to the region of interest. It was subsequently shown that super-resolution of $\sim\lambda/4$ is possible through detection of the field intensity in a reflection readout geometry.⁹

In this letter, we extend the investigation in Ref. 9 to study near field optical readout by detection of the *transmitted* field intensity. The aim is to achieve super-resolution through modulating the surface plasmon-enhanced transmission. There are several reasons a transmission readout system could offer more benefits than one based upon reflection. First, this allows for the surface plasmon-enhanced transmission to be exploited directly. Second, the amount of useful signal in the reflection configuration is relatively limited as backscattering in the vicinity of the subwavelength slit contributes significantly to the overall reflected field. Third, plasmon pits on the illuminated side of the metal plate, which degrade the readout contrast in the reflection readout configuration,⁸ can now be incorporated to enhance the transmission,¹⁰ directly increasing the strength of the signal. Finally, the detection geometry for the transmission configuration should be more straightforward to implement in practice.

We employed a Green’s tensor formulation that allows for an exact numerical solution to Maxwell’s equations¹¹ to simulate the propagation of electromagnetic waves and their interactions with the surface plasmons. The geometry of the

readout system is shown in Fig. 1. A metal plate (taken to be Ag) of thickness $t_2=100$ nm with a subwavelength slit of width $a=25$ nm is illuminated with an incident field, a Gaussian beam synthesized through the angular spectrum representation of plane waves. Its wavelength λ is taken to be 500 nm, and its beamwidth is 530 nm at full width at half maximum. Plasmon pits (40 nm wide and 40 nm deep) are located (in pairs) either only on the dark side or on both sides of the Ag plate. The distance between the plasmon pits on the dark and light sides is given by 2γ and $2\gamma'$, respectively. The data layer is separated from the metal plate by a distance $t_3=30$ nm, and its thickness is taken to be $t_4=30$ nm. The data pit is taken to be 40 nm wide and 15 nm deep. The choice of such a thin data layer reduces the effects of absorption and allows for possible plasmon-assisted field enhancement effects when the data layer is also metallic.^{12,13} We speculate that it would be possible also to achieve similar field enhancement effects with a dielectric data layer (such as Si) instead, but with metallic strips replacing the dielectric material where the air pits are present. In the discussion that follows, we will consider the data structure to be either a Ag layer with air pits or a Si layer embedded with strips of Ag, referring to them, respectively, as “Ag data layer” and “Si data layer.”

To quantify the readout performance, we defined the readout contrast as the percentage difference in the transmission T when the data structure is present and absent, i.e.,

$$\text{readout contrast} \equiv \frac{|T_{\text{data}} - T_{\text{nodata}}|}{|T_{\text{nodata}}|}. \quad (1)$$

In Eq. (1), the transmission T has been normalized to the incident field such that

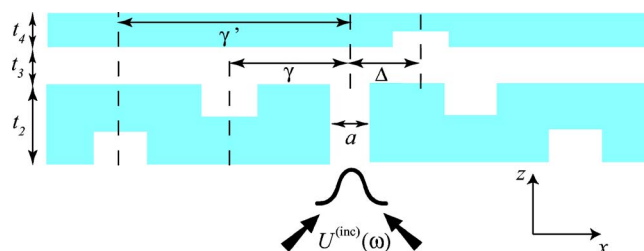


FIG. 1. (Color online) Illustration of the geometry.

^{a)}Electronic mail: chgan@uncc.edu

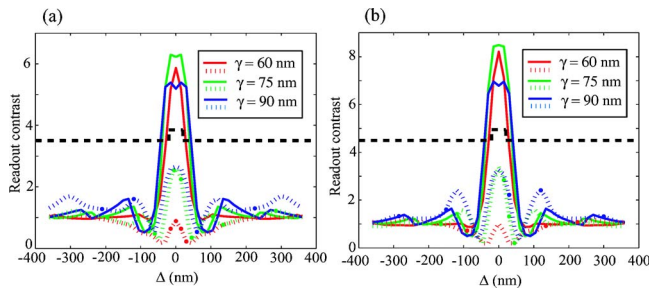


FIG. 2. (Color online) Readout contrast for one data pit (a) with $\gamma' = 225$ nm and (b) without light side plasmon pits. Solid lines are for Ag and dotted lines are for Si data layer. The black dashed line indicates the position of the data pit.

$$T = \frac{\int_{-\infty}^{+\infty} S_{z1} dx}{Y_0 \int_{-\infty}^{+\infty} |E^{(\text{inc})}(x, z)|^2 dx}, \quad (2)$$

where S_{z1} is the normal component of the time-average Poynting vector emerging from the data layer, $Y_0 = \sqrt{\epsilon_0/\mu_0}$, and $E^{(\text{inc})}(x, z)$ is the electric field amplitude of the incident Gaussian beam. The integral in the numerator of Eq. (2) implies capturing the total output power. This can be a concern, especially in experiments, if there is a lot of power scattered at highly oblique angles. To address this issue, we have also studied the far-field radiation patterns for the geometries considered. Our simulations revealed that the scattered power lies predominantly in the forward direction. As such, we have reason to believe that the system can capture the bulk of the transmitted optical power.

The choice of γ' is such as to obtain enhanced optical transmission through the slit. Numerical simulations with only the subwavelength slit and the light side plasmon pits (without the dark side plasmon pits and data layer) show that maximum transmission occurs at $\gamma' \sim 225$ nm. The choice of γ is determined through numerical simulations of the readout contrast for various values of γ with a single data pit. From previous findings in Refs. 8 and 9, we expect the dark side plasmon pits to aid both in confining the enhanced field effects to the vicinity around the data structure, and in suppressing undesirable oscillations of the transmission. Figure 2 shows that for either the Ag or Si data layer, the optimal value of γ is ~ 75 nm. It is worth noting that the analysis here yields very similar results to the reflection configuration,⁹ where the optimal value of γ was found to be ~ 80 nm.

The readout contrast defined in Eq. (1) does not provide information on the amount of transmission through the system. As such, we have also analyzed the distribution of the electric field intensity in the system (see Fig. 3). It can be observed that the field intensity through the Ag layer is more intense than that through the Si layer, even though Si is more transparent than Ag at $\lambda = 500$ nm. With $\gamma = 75$ nm and no plasmon pits on the light side, T_{nodata} through the Ag and Si data layers is 0.31% and 0.22%, respectively. When the light side plasmon pits are present, T_{nodata} increases to 1.33% and 1.06%. These simulations are repeated with the Ag plate replaced with a Si plate, and T_{nodata} was found to increase from 3.32% to 3.79% (Si data layer) and from 5.59% to 6.53% (Ag data layer). The higher value of T_{nodata} in the case of the 100 nm Si plate is expected due to the decrease in absorp-

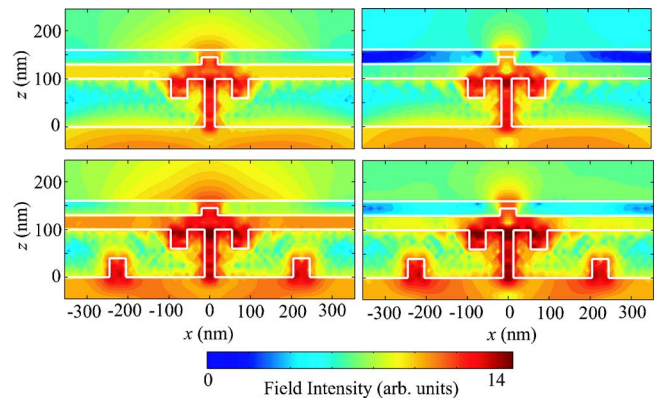


FIG. 3. (Color online) Field intensity distribution with and without light side plasmon pits: $\gamma = 75$ nm and $\gamma' = 225$ nm. Plots on the left column and right column for Ag and Si data layers, respectively.

tion, but clearly the transmission increases minutely in the presence of the light side plasmon pits. These results suggest the presence of surface plasmon-enhanced field effects through the Ag sections. While the Si data layer provides a lower readout contrast, the plots in Fig. 3 also show that the Ag strip embedded within is more effective in confining the surface-plasmon enhanced transmission in the near field, and has the potential to provide higher resolution.

For resolution, we have adopted a criterion more stringent than the Rayleigh criterion¹⁴ (Sec. 7.6.3). Two data pits are considered resolved when the transmission returns to T_{nodata} between two data pits. A closer examination of Fig. 2 shows that for the Si data layer, the transmission dips drastically when the edges of the data pit coincide with the center of the slit. This can arise from increased backscattering at the discontinuity along the Ag/Si/air boundaries. Such a backscattering mechanism, typically undesirable in many applications, offers the possibility to detect the edges of the data pits through the associated transmission minima. Detection of the edges is useful when binary data is encoded on the edges of the data pit, similar to the method in which conventional compact disks are encoded.¹⁵ However, on account of our definition for the readout contrast in Eq. (1), the maximum achievable readout contrast for edge detection is limited to unity; the transmission peaks play no role in edge detection, unlike in pit detection. We like to point out that the strategy to detect the edges differ from that in Ref. 9, where plasmon resonances at the edges had been exploited and a readout contrast of 700% was achieved. The reason we do not employ the same strategy here for edge detection is that the size of the data pit in the present study is 40×15 nm², smaller as compared to 50×25 nm² in the previous case,⁹ and therefore discriminating the plasmon resonances at each of the edge is significantly more challenging.

Based on the above discussion, the following strategies were investigated: (1) data pit detection with Ag data layer, (2) data pit detection with Si data layer, and (3) edge detection with Si data layer. For all three cases, the readout performance with and without the light side plasmon pits are compared to assess the overall improvement when the transmission is enhanced. The simulation results are shown in Fig. 4. For each configuration [(1), (2), and (3)], resolution up to 110 nm ($\lambda/4.5$), 90 nm ($\lambda/5.6$), and 180 nm ($\lambda/2.8$)

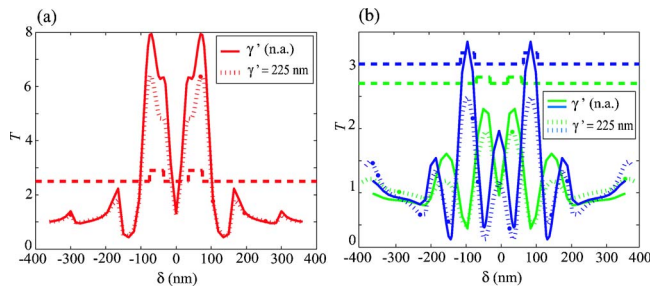


FIG. 4. (Color online) Readout contrast for two data pits: (a) pit detection in Ag data layer and (b) pit detection (green) and edge detection (blue) in Si data layer. δ is the distance between the location midway of the two data pits and the subwavelength slit; the slit coincides with the data pit at $\delta = \pm \Delta$, with $\Delta = \text{DPS}/2$ (DPS: data pit separation). The solid lines show the results without light side plasmon pits [γ' not applicable (n.a.)]. The dashed lines indicate the respective positions of the data pits.

was obtained, with readout contrast of around 600%, 200%, and 60%, respectively.

The Si layer provides better resolution for data pit detection, an effect we attribute to the more effective localization of the field enhancement effects. This better localization is achieved at the expense of the enhanced transmission T_{data} , leading to the lower readout contrast. Edge detection doubles the features to be detected, and it was therefore not unreasonable for the resolution to be inferior.

In summary, we have demonstrated numerically that with careful selection of system parameters, surface plasmon-enhanced transmission can be manipulated to achieve super-resolution in near field optical readout. Our simulations suggest that it is possible to optimize the application of these plasmonic effects by modulating them with a corrugated metal film or a dielectric film embedded with metal strips. In the strategies simulated, super-resolution of

data structures up to $\sim \lambda/5$ is possible. We have shown that different kinds of plasmon-assisted transmission effects can be combined to optimize performance in an application. We hope that these results would lead to the effective employment of surface plasmon-enhanced transmission for optical readout and other near field applications.

This research was supported by the Department of Energy under Grant No. DE-FG02-06ER46329.

- ¹J. Tominaga, T. Nakano, and N. Atoda, Appl. Phys. Lett. **73**, 2078 (1998).
- ²T. Nakano, A. Sato, H. Fuji, J. Tominaga, and N. Atoda, Appl. Phys. Lett. **75**, 151 (1999).
- ³Q. Chen, J. Tominaga, L. Men, T. Fukaya, N. Atoda, and H. Fuji, Opt. Lett. **26**, 274 (2001).
- ⁴H. S. Lee, B. Cheong, T. S. Lee, K. S. Lee, W. M. Kim, J. W. Lee, S. H. Cho, and J. Y. Huh, Appl. Phys. Lett. **85**, 2782 (2004).
- ⁵T. W. Ebbesen, H. J. Lezec, H. F. Ghaemi, T. Thio, and P. A. Wolff, Nature (London) **391**, 667 (1998).
- ⁶T. Thio, K. M. Pellerin, R. A. Linke, H. J. Lezec, and T. W. Ebbesen, Opt. Lett. **26**, 1972 (2001).
- ⁷*Optical Nanotechnologies: The Manipulation of Surface and Local Plasmons*, edited by J. Tominaga and D. P. Tsai (Springer, Heidelberg, 2003).
- ⁸G. Gbur, H. F. Schouten, and T. D. Visser, Appl. Phys. Lett. **87**, 191109 (2005).
- ⁹C. H. Gan and G. Gbur, Opt. Express **14**, 2385 (2006).
- ¹⁰F. J. García-Vidal, H. J. Lezec, T. W. Ebbesen, and L. Martín-Moreno, Phys. Rev. Lett. **90**, 213901 (2003).
- ¹¹T. D. Visser, H. Blok, and D. Lenstra, IEEE J. Quantum Electron. **35**, 240 (1999).
- ¹²N. Bonod, S. Enoch, L. Li, E. Popov, and M. Nevière, Opt. Express **11**, 482 (2003).
- ¹³A. Giannattasio, I. R. Hooper, and W. L. Barnes, Opt. Express **12**, 5881 (2004).
- ¹⁴M. Born and E. Wolf, *Principles of Optics*, 7th ed. (Cambridge University Press, Cambridge, 1999).
- ¹⁵K. C. Pohlmann, *The Compact Disc Handbook*, 2nd ed. (Oxford University Press, Oxford, 1992).